J Physiol 590.7 (2012) pp 1517–1534

The Journal of Physiology

TECHNIQUES FOR PHYSIOLOGY

Virus-mediated swapping of zolpidem-insensitive with zolpidem-sensitive $GABA_A$ receptors in cortical pyramidal cells

Mate Sumegi[1,2], Yugo Fukazawa[1,3], Ko Matsui[1,3,4], Andrea Lorincz[2], Mark D. Eyre[2], Zoltan Nusser[2] and Ryuichi Shigemoto[1,3,5]

[1]*Division of Cerebral Structure, National Institute for Physiological Sciences, Okazaki 444-8787, Japan*
[2]*Laboratory of Cellular Neurophysiology, Institute of Experimental Medicine, Hungarian Academy of Sciences, 1083 Budapest, Hungary*
[3]*Department of Physiological Sciences, Graduate University for Advanced Studies (SOKENDAI), and* [4]*PRESTO and* [5]*SORST, Japan Science and Technology Agency, Kawaguchi 333-0012, Japan*

Key points

- We generated lenti- and adeno-associated viruses which were used to replace the zolpidem-insensitive $GABA_A$ receptors of a transgenic mouse line with wild-type, zolpidem-sensitive ones.
- The virally expressed wild-type, zolpidem-sensitive $GABA_A$ receptor $\gamma 2$ subunits were tagged with a small immunotag (AU1).
- Light microscopic fluorescent and electron microscopic freeze-fracture immunogold labelling revealed that the virally introduced AU1-tagged $\gamma 2$ subunit-containing receptors had a normal synaptic distribution on cortical pyramidal cells.
- *In vitro* patch-clamp recordings demonstrated that the insertion of this immunotag did not alter the kinetic and pharmacological properties of the virally inserted $\gamma 2$ subunits.
- Our results demonstrate a novel transgenic–viral pharmacogenetic approach, which allows the selective silencing of well-defined neuronal populations in the brain.

Abstract Recently developed pharmacogenetic and optogenetic approaches, with their own advantages and disadvantages, have become indispensable tools in modern neuroscience. Here, we employed a previously described knock-in mouse line ($GABA_AR\gamma 2^{77I}$lox) in which the $\gamma 2$ subunit of the $GABA_A$ receptor ($GABA_AR$) was mutated to become zolpidem insensitive ($\gamma 2^{77I}$) and used viral vectors to swap $\gamma 2^{77I}$ with wild-type, zolpidem-sensitive $\gamma 2$ subunits ($\gamma 2^{77F}$). The verification of unaltered density and subcellular distribution of the virally introduced $\gamma 2$ subunits requires their selective labelling. For this we generated six N- and six C-terminal-tagged $\gamma 2$ subunits, with which cortical cultures of $GABA_AR\gamma 2^{-/-}$ mice were transduced using lentiviruses. We found that the N-terminal AU1 tag resulted in excellent immunodetection and unimpaired synaptic localization. Unaltered kinetic properties of the AU1-tagged $\gamma 2$ ($^{AU1}\gamma 2^{77F}$) channels were demonstrated with whole-cell patch-clamp recordings of spontaneous IPSCs from cultured cells. Next, we carried out stereotaxic injections of lenti- and adeno-associated viruses containing Cre-recombinase and the $^{AU1}\gamma 2^{77F}$ subunit (Cre-2A-$^{AU1}\gamma 2^{77F}$) into the neocortex of $GABA_AR\gamma 2^{77I}$lox mice. Light microscopic immunofluorescence and electron microscopic freeze-fracture replica immunogold labelling demonstrated the efficient immunodetection of the AU1 tag and the normal enrichment of the $^{AU1}\gamma 2^{77F}$ subunits in perisomatic GABAergic synapses. In line with this, miniature and action potential-evoked IPSCs whole-cell recorded from

DOI: 10.1113/jphysiol.2012.227538

transduced cells had unaltered amplitudes, kinetics and restored zolpidem sensitivity. Our results obtained with a wide range of structural and functional verification methods reveal unaltered subcellular distributions and functional properties of $\gamma2^{77I}$ and $^{AU1}\gamma2^{77F}$ $GABA_ARs$ in cortical pyramidal cells. This transgenic–viral pharmacogenetic approach has the advantage that it does not require any extrinsic protein that might endow some unforeseen alterations of the genetically modified cells. In addition, this virus-based approach opens up the possibility of modifying multiple cell types in distinct brain regions and performing alternative recombination-based intersectional genetic manipulations.

(Received 5 January 2012; accepted after revision 15 February 2012; first published online 20 February 2012)
Corresponding author Z. Nusser: Laboratory of Cellular Neurophysiology, Institute of Experimental Medicine, Hungarian Academy of Sciences, Szigony Street 43, 1083 Budapest, Hungary. Email: nusser@koki.hu

Abbreviations BZ, benzodiazepine; eGFP, enhanced green fluorescent protein; $GABA_AR$, type-A GABA receptor; LM, light microscopic; PC, pyramidal cell; RE, restriction endonuclease; SDS-FRL, sodium dodecyl sulphate-digested freeze-fracture replica-labelling.

Introduction

In recent years, a number of different approaches have been described that allow the selective pharmacological modification of the activity of genetically modified cell populations. These methods have already contributed enormously to our understanding of the role of defined cell populations in certain behaviours (Callaway, 2005). One of the first pharmacogenetic approaches was developed by Lester *et al.* who either virally (Slimko *et al.* 2002) or transgenically (Lerchner *et al.* 2007) introduced invertebrate ivermectin-sensitive Cl^- channels into mammalian neurons and demonstrated their efficient hyperpolarization with exogenously applied low concentrations of ivermectin. A similar approach using the *Drosophila* G-protein-coupled allatostatin receptor (AlstR) was developed for reversible and transient inhibition of neurons (Lechner *et al.* 2002; Tan *et al.* 2006). Although allatostatin has no effect on mammalian neurons and efficiently hyperpolarizes AlstR-expressing neurons, a major weakness of this approach is the lack of penetration of the ligand through the blood–brain barrier. An alternative approach is the use of so-called designer receptors, which are mutated versions of, for example, the human muscarinic receptor (hM4D) that are made sensitive to a pharmacologically inert drug (clozapine-*N*-oxide: CNO; Armbruster *et al.* 2007; Ferguson *et al.* 2011) and are made insensitive to their endogenous ligands. The application of CNO exerts its effect on neuronal excitability by activating the designer receptor and consequently the endogenously expressed Kir3 K^+ channels. A very similar approach was taken by Magnus *et al.* (2011) who modified ligand-gated ion channels to endow selectivity to inert ligands. They generated chimeras of the $\alpha7$ nicotinic and glycine receptors with point mutations in the ligand-binding domains of the $\alpha7$ subunit to make it insensitive to endogenous ligand and sensitive to an inert drug, the application of which produced a pronounced hyperpolarization of the chimeric receptor-expressing cells. Although these methods rely on the activation of either K^+ or Cl^- channels, they have one common feature: they are all based on the genetic introduction of exogenous proteins. How these proteins interfere with the translation/assembly/processing of other proteins at the level of the endoplasmic reticulum/Golgi apparatus and how they influence the neurons' intrinsic excitability when they are present in the plasma membrane are largely unknown, but impose potential unforeseen problems.

A fundamentally different pharmacogenetic approach was developed by Wulff *et al.* (2007) who generated a knock-in mouse line ($GABA_AR\gamma2^{77I}$lox) in which the 77th amino acid of the $GABA_A$ receptor ($GABA_AR$) $\gamma2$ subunit was mutated from phenylalanine ($\gamma2^{77F}$) to isoleucine ($\gamma2^{77I}$) and the mutated receptor gene was flanked by two LoxP sites. This mutation renders the composed $GABA_ARs$ insensitive to zolpidem, a benzodiazepine (BZ) site ligand, and affects every $\gamma2$ subunit in every neuron of the brain, making the whole animal zolpidem insensitive. Importantly, this single amino acid mutation did not change the subcellular distribution or the kinetic properties of the $GABA_ARs$. Wulff *et al.* (2007) generated two additional transgenic mouse lines; in the first one the Purkinje cell-specific L7 promoter drove the expression of Cre-recombinase and in the second one it drove the expression of the $\gamma2^{77F}$ subunit. By crossing these three genetically modified mouse lines, they swapped zolpidem-insensitive with zolpidem-sensitive $GABA_ARs$ only in cerebellar Purkinje cells and showed that GABAergic inhibition was potentiated only in Purkinje cells following the administration of zolpidem in these animals. Another elegant aspect of this method is that GABAergic synaptic currents can be reduced by BZ site inverse agonists (e.g. β-carbolines DMCM and β-CCM), resulting in a selective increase in the excitability of the targeted cells. Another major advantage of this approach

is the lack of exogenous protein expression in nerve cells, eliminating the possibility of unwanted effects. However, the major disadvantage of the methods described by Wulff *et al.* (2007) was the necessity of generating many transgenic mouse lines and potential alterations in the developmental expression of $\gamma2^{77F}$ caused by the L7 promoter. If a single viral vector could accommodate both Cre-recombinase and $\gamma2^{77F}$, one could stereotaxically inject it into certain brain areas of $GABA_AR\gamma2^{77I}$lox mice to enable negative and positive allosteric modulation of the transduced cells. The effects of transient and reversible negative and positive allosteric modulation of inhibition on the transduced cells with blood–brain barrier-penetrating pharmacological agents could then be analysed at the system and behavioural levels. In the present manuscript, we describe the generation of lenti- and adeno-associated viruses expressing Cre-recombinase and N-terminal AU1-tagged $\gamma2^{77F}$ subunits and employ light- and electron microscopic immunolocalization as well as *in vitro* electrophysiological methods to verify the unaltered subcellular and synaptic locations and kinetic properties of the virally inserted $GABA_A$Rs.

Methods

Tagging the $GABA_AR$ $\gamma2$ subunit

The original $GABA_A$ receptor $\gamma2$-L subunit cDNA (pRK5$\gamma2$-L, gift from Drs Peer Wulf and William Wisden) was modified by inserting a BamHI recognition site in front of the signal peptide's start codon. The enhanced green fluorescent protein (eGFP) sequence in the pFUGW (Lois *et al.* 2002) lentiviral backbone plasmid was replaced by inserting the BamHI-BstEII fragment of the modifed pRK5$\gamma2$-L between the BamHI and the EcoRI sites of the lentiviral plasmid, resulting in pF-U-[$\gamma2$]W. For the tag insertions, the $\gamma2$-L subunit cDNA was subcloned into pBSKSII(+), and an internal removable insert was placed between the 4th and 5th amino acid residue of the mature protein (referred to as N-terminal position) or at the C-terminus (Fig. 1). PCR primers used for N-terminal insertions were (TTGAATTCTCAGTCAGATGATGACTATGAAGATTAC ACTTCTAAT), (TTGAATTCCTCTAGTCATCATCTGAC TTTTGGCTTGTG). Those for the C-terminal insertions were, (CTGGGGAATTCTCTTTATCTGTAAAGAGGTAT GGGTTTTATTGATA) and (ATAGTGAATTCCTCATAC CTCTCAGATAAAGATAGGAGACCCAGTAAACAAGAT TGAAC). The removable inserts were then replaced with the tag coding synthetic double-stranded oligo-nucleotides and the tagged subunits were cloned back to the pF-U-[$\gamma2$]W construct. The amino acid sequences of the tags were AU1: DTYRYI; BBS (α-bungarotoxin binding site): WRYYESSLEPYPD; FLAG: DYKDDDDK; 3XFLAG: DYKDHDGDYKDHD IDYKDDDDK; HA: YP YDVPDYA; STREP II: WSHPQFEK.

Generation of pF-U-[Cre]W, pF-U-[Cre-2A-$^{AU1}\gamma2$]W and pAAV-CMV-[Cre-2A-$^{AU1}\gamma2$]W-SV40pA viral plasmids

The nls-Cre recombinase was first removed from the pPGK-Cre-bpA plasmid (Addgene plasmid 11543) by SalI, MluI digestion and ligated into a modified pBSKSII(+) plasmid containing the MluI, HindIII, SalI, BglII sites between the EcoRI and XhoI sites of the original Multi Cloning site (MCS). Later the EcoRI, BglII fragment of the resulting plasmid was used to replace the EcoRI, BamHI fragment of the pFUGW plasmid to generate the pF-U-[Cre]W. For the generation of the pF-U-[Cre-2A-$^{AU1}\gamma2$]W, first the PshAI,Van91I fragment of the pF-U-[Cre]W plasmid was replaced with a synthetic DNA fragment coding the last 65 amino acid residues of the Cre recombinase without the stop codon, followed by the in-frame addition of a picorna virus 2A-like peptide (KQKIVAPVKQTLNFDLLKLAGDVESNPGP) coding sequence (Donnelly *et al.* 2001) and the first 10 basepairs of the $\gamma2$-L cDNA. The 3′ terminus of the $\gamma2$-L cDNA was later completed by inserting the BstXI,Van91I fragment of the pF-U-[$^{AU1}\gamma2$]W plasmid between the BstXI,Van91I sites. For AAV backbone plasmid generation the neomycin expression cassette of the pTR-eGFP plasmid (from Dr Samulski, University of North Carolina) was deleted and the eGFP coding region was replaced with the [Cre-2A-$^{AU1}\gamma2$]W region of the pF-U-[Cre-2A-$^{AU1}\gamma2$]W plasmid.

Virus production

Viral vectors were produced by transient transfection of cells from the human embryonic kidney cell line 293T, with a protocol modified from Naldini *et al.* (1996). Briefly, a total of 5×10^6 293T cells were seeded in 10 cm diameter poly-L-lysine-coated dishes in 5 ml Dulbecco's modified Eagle's medium (D-MEM)-high glucose (Sigma)–10% fetal calf serum (FCS) (Sigma) in a humidified 5% CO_2 incubator at 37°C 24 h prior to transfection. The culture medium was changed with 10 ml fresh medium 1 h prior to transfection. Five micrograms of envelope plasmid (pCMV-VSV-G) and 5 μg packaging plasmid (pCMV-HIVgpΔ8.9), both kindly provided by Dr Pavel Osten at the Max Planck Institute, and 5 μg lentiviral backbone plasmid were used for each transfection. The three plasmids were mixed in water (to 870 μl final volume) and left at 4°C overnight. On the following day 130 μl of a 2 M $CaCl_2$ solution was added to the DNA solution, mixed and 1 ml of Hepes-buffered saline (281 mM NaCl, 50 mM Hepes, 1.5 mM Na_2HPO_4; pH = 7.22) was slowly added during constant mixing. The freshly formed precipitate was immediately added to the cultures. After 16 h,

the transfection medium was replaced with 10 ml fresh medium supplemented with 20 μl of 1 mg ml^{-1} forskolin (Sigma) dissolved in DMSO (Sigma). The supernatant was collected one day later, then cleared by low-speed centrifugation and filtered through a 0.45 μm PVDF membrane (Millipore). Concentration was achieved by ultracentrifugation at 50,000 *g*, 4°C for 2 h, followed by re-suspension in 900 μl Hank's balanced salt solution (HBSS), layering on top of 1 ml of 20% sucrose cushion and centrifuged at 53,000 *g*, 4°C for 2 h. The pellet was re-suspended in 100 μl calcium- and magnesium-free (CMF)-HBSS, kept in the centrifuge tube overnight at 4°C, aliquoted, snap-frozen in liquid nitrogen and stored at –80°C. The titre of some virus preparations was assayed by a HIV-1 p24 ELISA kit (PerkinElmer). One nanogram of p24 group-specific antigen (gag) protein was considered to represent 5000 infectious units (IU) and most virus preparations used in the present study had titres of $>10^5$ IU μl^{-1}. AAV-2 virus particles pseudo-coated with AAV-9 cap proteins (4.6×10^{12} GC ml^{-1}) were generated in the Penn Vector Core, University of Pennsylvania.

$GABA_AR\gamma2^{-/-}$ mice and genotyping the embryos

C57BL/6 mice heterozygous for the $GABA_A$ receptor $\gamma2$ subunit ($\gamma2^{-/+}$; Günther *et al.* 1995; kindly provided by Dr Bernhard Luscher) were raised on a 12 h light/dark cycle with water and food *ad libitum* and crossed to obtain embryonic day (E)16 embryos. All the animal experiments were conducted in accordance with the guidelines of the National Institute for Physiological Science's Animal Care and Use Committee. The embryos used for primary neuronal cultures were genotyped during the process of cell culturing and for most experiments only the cells from $\gamma2^{-/-}$ embryos were plated. Two legs were isolated from each embryo, one was kept at –80°C for subsequent confirmation of the genotype. Another leg was used for quick genotyping using a method modified from McClive & Sinclair (2001). Briefly, legs were washed twice in distilled water and once in DB-K (Digestion Buffer without Proteinase-K) (50 mM KCl, 19 mM Tris-HCl; pH = 8.3, 0.1 mg ml^{-1} gelatin, 0.45% NP40, 0.45% Tween-20), then incubated in 50 μl DB (Digestion Buffer) (DB-K + 60 U ml^{-1} proteinase-K) at 55°C for 5 min. Proteinase-K was inactivated by incubation at 95°C for 10 min followed by a brief vortexing. The undigested tissue was sedimented by a centrifugation for 20 s at 14,000 *g*. One microlitre of the supernatant was used in a 31.5 μl PCR reaction (1x Takara PCR reaction buffer, 0.2 mM dNTPs, 250 nM primers, 0.79 U Takara-Taq), applying the following programme: 1 s at 98°C, 30 s at 60°C, 2 min at 72°C, repeated 28 times. The PCR primers were: CATCTCCATCGCTAAGAATGTTCGGGAAGT ($\gamma2^{-/+}$), ATGCTCCAGACTGCCTTGGGAAAAGC ($\gamma2^{-}$) and GCTGACAAAATAATGCAGGGTGCCATACTC ($\gamma2^{+}$). The PCR products were subjected to an electrophoresis at high current (300 mA, 4°C) for ~12 min. The genotype of the embryos selected for the primary culture was further confirmed later by a conventional DNA isolation (DNeasy Blood and Tissue Isolating Kit, Qiagen), followed by a similar PCR and conventional gel electrophoresis.

Primary cortical neuronal cultures

Primary cultures of cortical neurons were prepared from mouse embryos (E16). Pregnant mice were killed by cervical dislocation. The embryos were immediately dissected and placed in ice-cold CMF-HBSS (Gibco). The brains were removed from individual embryos and the neocortex was isolated and cut into small pieces. The tissue was collected into a 15 ml tube and sedimented by low-speed centrifugation (800 *g*, 1 min). The supernatant was replaced with 2 ml 0.25% trypsin (Gibco) and 4 mg ml^{-1} DNase I in CMF-HBSS and incubated at 37°C for 15 min, with gentle agitation every 3 min. Enzymatic dissociation was stopped by adding 0.8 ml FCS and cells were physically dissociated by triturating with a pipette. After that, 5 ml of MEM+ (Minimum Essential Media) solution was added (5% FCS, 2% B-27 supplement (Gibco), 50 mM L-glutamate (Gibco) and 92.75% MEM (200 mg l^{-1} $CaCl_2$, 400 mg l^{-1} KCl, 200 mg l^{-1} $MgSO_4$, 6.8 g l^{-1} NaCl, 2.2 g l^{-1} $NaHCO_3$, 158 mg l^{-1} $NaH_2PO_4.2H_2O$, 7 g l^{-1} D-glucose, 0.5 mg l^{-1} choline chloride, 0.5 mg l^{-1} D-calcium pantothenate, 0.5 mg l^{-1} folic acid, 0.5 mg l^{-1} i-inositol, 0.9 mg l^{-1} nicotinamide, 0.5 mg l^{-1} pyridoxal hydrochloride, 0.5 mg l^{-1} thiamine hydrochloride, 0.04 mg l^{-1} riboflavine, 1x MEM amino acid solution, 100 U l^{-1} penicillin–100 μg l^{-1} streptomycin, 15 mM Hepes (pH = 7.25)), briefly mixed and centrifuged for 10 min at 180 *g* at 4°C. The pellet was re-suspended in 3 ml MEM+, filtered through a cell strainer (100 μm, Becton, Dickinson and Company, Franklin Lakes, NJ, USA) and diluted in MEM+ to a final concentration of 9×10^4 cells ml^{-1}. Cells from $\gamma2^{-/-}$ and $\gamma2^{+/+}$ embryos (1.8×10^4 cells/dish) were seeded onto poly-L-lysine-coated glass-bottomed 35 mm cell culture dishes (Iwaki, Tokyo, Japan) and cultured at 37°C in a humidified 5% CO_2 atmosphere. For electrophysiological experiments, cells were seeded onto 35 mm cell culture dishes containing poly-L-lysine-coated coverslips (Matsunami, Osaka, Japan). After 4 h of incubation 1–2.5 μl of lentiviral vector was added to the cultures. All chemicals and reagents were obtained from Sigma, unless otherwise stated.

Immunohistochemistry on neuronal cultures

Immunoreactions were performed on cells cultured for 19–27 DIV. Cells were fixed with 10% paraformaldehyde

for 30 min at 37°C, washed in PBS, and blocked with PBS containing 0.1% Triton X-100 and 5% normal goat serum (PBST-NGS). The cells were then incubated at 4°C in PBST-NGS containing the primary antibodies for 16 h. The following primary antibodies were used: rabbit anti-γ2 subunit (1:500; gift from Prof. Werner Sieghart), mouse anti-β2/3 subunit (Millipore Corporation, Billerica, MA, USA; MAB341), mouse anti-AU1 (1:5000; Covance Inc., Princeton, NJ, USA; MMS-130R), mouse anti-Flag M2 (1:500–2500; Sigma F3165), mouse anti-HA (1:500; Abcam Inc., Cambridge, MA, USA; 12CA5, ab16918) and mouse anti-Strep-tag II (1:500; IBA GmbH, Gottingen, Germany, 21507001). After washing, the cells were incubated in secondary antibodies: Alexa488-conjugated goat anti-mouse IgG (Invitrogen, A11029), or Alexa594-conjugated goat anti-rabbit IgG (Invitrogen, A11037), or Alexa488-conjugated bungarotoxin (1:500; Invitrogen B13422). Finally, the cells were washed in PBS and were mounted in Vectashield (Vector Laboratories, Burlingame, CA, USA).

In vitro whole-cell patch-clamp recording of mIPSCs from cultured cortical neurons

Dissociated cells were prepared as described above, cultured for 19–33 DIV and used for electrophysiological examination of mIPSCs. Cells cultured on coverslips were transferred to the recording chamber and superfused continuously at room temperature with a solution containing (in mM): 119.0 NaCl, 2.5 KCl, 2.0 $CaCl_2$, 1.3 $MgCl_2$, 1.0 NaH_2PO_4, 26.2 $NaHCO_3$, and 11.0 glucose (saturated with 95% O_2 and 5% CO_2). Cells were visualized using a ×60 water-immersion objective on a BX51WI upright microscope (Olympus, Tokyo, Japan). Whole-cell recordings were made with an Axopatch 200B amplifier (Molecular Devices, Sunnyvale, CA, USA), signals were filtered at 2 kHz, digitized at 10 kHz with Digidata 1440A interface and collected using pCLAMP 10 acquisition software (Molecular Devices). The pipette solution contained (in mM): 60 $CsCH_3SO_3$, 60 CsCl, 10 Hepes, 10 EGTA, 4 $MgCl_2$, 4 ATP, 0.5 GTP and were titrated to pH 7.2 with CsOH. Recorded cells were voltage clamped at −68 mV, and as the equilibrium potential for Cl^- with the above solutions was calculated as −16 mV, IPSCs appeared as inward currents. TTX (0.5 μM), CNQX (5 μM) and DL-AP5 (50 μM) (all from Tocris Bioscience, Bristol, UK) were added to the superfusate to block action potentials, AMPA receptors, and NMDA receptors, respectively. Zolpidem (1 μM) (Sigma) and SR95531 (30 μM) (Tocris Bioscience) were used. Data analysis was performed using AxoGraph X (AxoGraph Scientific, Sydney, Australia), and statistical analysis was performed using Microsoft Excel (Microsoft, Redmond, WA, USA) and StatView (SAS Institute, Cary, NC, USA). Time from 20% to 80% of the peak amplitude was measured as rise time, and time to decay to 1/e times the peak amplitude was taken as decay time.

Lentiviral injections

Male $GABA_AR\gamma2^{77I}$lox mice between 1 and 7 months old were anaesthetized with ketamine:piplophen:xylazine (62.5:6.25:12.5 μg (g body weight)$^{-1}$) and ∼0.6 μl lentivirus solution was stereotaxically injected into the neocortex at 0.1 μl min^{-1} flow rate. The animals were kept in ABSL-2 containment for at least 2 weeks before further use. All procedures were carried out in accordance with the ethical guidelines of the Institute of Experimental Medicine of the Hungarian Academy of Sciences, which is in line with the European Union regulations on animal experimentation.

Immunofluorescence reactions on brain sections

Two to ten weeks after the lentiviral injections adult male $GABA_AR\gamma2^{77I}$lox mice (1–7 months old; bred in the Institute of Experimental Medicine's Animal facility; C57BL/6) were deeply anaesthetized with ketamine before transcardial perfusion with ice-cold fixative. Mice were perfused with fixatives containing 4% paraformaldehyde in 0.1 M sodium phosphate buffer (PB, pH = 7.3) or in 2% paraformaldehyde in 0.1 M sodium acetate (pH = 6) buffer for 15 min. Coronal sections, 60 μm thick, were cut from the forebrain. Sections were then blocked in 10% normal goat serum (NGS) made up in Tris-buffered saline (TBS, pH = 7.4), followed by incubations in primary antibodies diluted in TBS containing 2% NGS and 0.1% Triton X-100. The following primary antibodies were used: rabbit anti-AU1 (1:1000; Abcam), mouse anti-AU1 (1:500; Covance), mouse anti-Cre (1:5000; Millipore), rabbit anti-Cre (1:1000; Covance), mouse anti-Kv2.1 (1:1000; Millipore), mouse anti-gephyrin (1:1000; SYSY, Göttingen, Germany), rabbit anti-green fluorescent protein (anti-GFP) (1:1000; Invitrogen), guinea pig anti-γ2 (1:1000; gift from Prof. J.-M. Fritschy) and rabbit anti-γ2 (1:1000; SYSY). The following secondary antibodies were used to visualize the immunoreactions: Alexa488-conjugated goat anti-rabbit and anti-mouse (1:1000; Invitrogen), Cy3-conjugated goat anti-rabbit, anti-mouse and donkey anti-guinea pig (1:1000, Jackson ImmunoResearch Europe Ltd, Newmarket, UK) IgGs.

Image acquisition

Immunofluorescence labelling was visualized by an inverted confocal scanning microscope (FV300, Olympus Co., Tokyo, Japan) using a ×40 (NA = 0.75) objective or with an upright confocal scanning laser microscope

(FV1000, Olympus) using a ×60 objective (NA = 1.35). Sequential acquisition of multiple channels was used for multi-colour images to avoid spectral crosstalk between channels.

SDS-digested freeze-fracture replica-labelling (SDS-FRL)

For SDS-FRL five adult (1–7 months old) male $GABA_AR\gamma2^{77I}$lox mice were injected with either a mixture of Cre-recombinase and eGFP or a mixture of Cre-2A-$^{AU1}\gamma2^{77F}$ and eGFP-expressing lentiviruses. Two to ten weeks after the injections mice were perfused with a fixative containing 2% paraformaldehyde in 0.1 M PB for 15 min. Coronal sections, 80 μm thick, were cut from the neocortex. Small blocks containing the injected area indicated by the endogenous eGFP fluorescence were cut out in such a way that the injection site dominated the centre of the block surrounded by a small non-injected area. Blocks were high pressure frozen and replicas were prepared as described earlier (Lorincz & Nusser, 2010). Tissue debris was digested from the replicas with gentle stirring in a TBS solution containing 2.5% SDS and 20% sucrose (pH = 8.3) at 80°C overnight. The replicas were blocked with 5% bovine serum albumin (BSA) in TBS for one hour. This was followed by an overnight incubation in TBS containing 1% BSA and the following primary antibodies: rabbit anti-AU1 (1:300; Abcam), rabbit anti-neuroligin-2 (1:1000; SYSY), mouse anti-β3 (1:1000; NeuroMab, UC Davis, CA, USA), guinea pig anti-γ2 (1:600; gift from Prof. J.-M. Fritschy) IgGs. Replicas were then incubated in TBS containing 5% BSA and the following secondary antibodies: goat anti-rabbit IgGs coupled to 10 nm gold particles, goat anti-mouse IgGs coupled to 15 nm gold particles, and goat anti-guinea pig IgGs coupled to 15 nm gold particles (all in 1:100; all from British Biocell International, Cardiff, UK). Replicas were rinsed in TBS and distilled water before they were picked up on copper parallel bar grids and examined with a transmission electron microscope (JEM-1011, JEOL Ltd, Tokyo, Japan) equipped with a high-resolution bottom-mounted CCD camera (Cantega G2, Olympus Soft Imaging Solution GmbH, Munster, Germany).

Acute slice preparation

Two weeks after virus injection, $GABA_AR\gamma2^{77I}$lox mice were deeply anaesthetized with isoflurane in accordance with the ethical guidelines of the Institute of Experimental Medicine Protection of Research Subjects Committee. After decapitation, the brain was removed and placed into ice-cold artificial cerebrospinal fluid (ACSF) containing (in mM): 230 sucrose, 2.5 KCl, 25 glucose, 1.25 NaH_2PO_4, 24 $NaHCO_3$, 4 $MgCl_2$ and 0.5 $CaCl_2$. Coronal slices from the cerebral cortex were cut at 250 μm thickness with a Vibratome (Leica VT1200S; Leica Microsystems) and were stored in ACSF containing (in mM): 126 NaCl, 2.5 KCl, 25 glucose, 1.25 NaH_2PO_4, 24 $NaHCO_3$, 2 $MgCl_2$ and 2 $CaCl_2$. All extracellular solutions were bubbled continuously with 95% O_2 and 5% CO_2, resulting in a pH of 7.4. After a 30 min recovery period at 33°C, slices were further incubated at room temperature until they were transferred to the recording chamber.

Electrophysiological recordings from acute slices and data analysis

Somatic whole-cell recordings were performed at 26.0 ± 0.9°C using IR-DIC on an Olympus BX51WI microscope with a ×40 water immersion objective. Recordings were carried out using a mixed potassium gluconate- and KCl-based intracellular solution (containing in mM: 65 potassium gluconate, 70 KCl, 2.5 NaCl, 1.5 $MgCl_2$, 0.025 EGTA, 10 Hepes, 2 Mg-ATP, 0.4 Mg-GTP, 10 creatinine phosphate, and 8 biocytin; pH = 7.33; 270–290 mosmol l^{-1}). Voltage-clamp recordings of mIPSCs at a holding potential of –70 mV were carried out in the presence of 1 μM TTX (Alomone Labs, Jerusalem, Israel) to block voltage-gated sodium channels and 3 mM kynurenic acid to inhibit ionotropic glutamate receptors. For animals injected with the lenti- or adeno-associated viruses containing Cre-2A-$^{AU1}\gamma2^{77F}$ the effects of 1 μM zolpidem was also tested. For paired recordings, TTX was omitted from the ACSF, and the same intracellular solution was used for both cells. Cells were held in whole-cell current-clamp mode, and a sequence of hyper- and depolarizing current injections were used to determine firing parameters. The putative postsynaptic pyramidal cell was then recorded in voltage-clamp mode whilst brief (1–3 ms) depolarizing currents were injected into the putative presynaptic fast-spiking basket cell every 3 s. Recordings were performed with a MultiClamp 700B amplifier (Molecular Devices). Data were digitized on-line at 20 kHz and filtered at 3 kHz with a low-pass Bessel filter. Individual mIPSCs were detected and analysed off-line with EVAN 1.5 (Nusser *et al*. 2001). Access resistance (R_a) was subject to 70% compensation and was continuously monitored. If R_a changed >20% during the recording, the cell was discarded from the analysis. All recordings were rejected if the uncompensated R_a became >20 MΩ.

Visualization of the recorded cells

After recordings, slices were fixed in 2% paraformaldehyde with 15% picric acid in 0.1 M PB for 24 h and then extensively washed with PB and TBS before re-sectioning at 60 μm thickness. Sections were blocked in TBS with 10% NGS for 1 h, and then incubated overnight in

mouse anti-Cre primary antibody (Millipore) diluted 1:5000 in TBS containing 0.1% Triton X-100 and 2% NGS. Sections were then washed in TBS and incubated in TBS containing Cy5-conjugated goat anti-mouse secondary antibody (Jackson ImmunoResearch) diluted 1:500 and streptavidin-conjugated Cy3 diluted 1:1000 (Jackson ImmunoResearch) to visualize the recorded cell. Slices were then washed in TBS, mounted and viewed using an Olympus FV1000 confocal microscope.

Results

Generation and testing different immuno- and affinity-tagged $GABA_A$ receptor $\gamma 2$ subunits

Thorough verification of the unaltered subcellular distribution and synaptic density of the virally introduced $\gamma 2^{77F}$ requires it to be identified and distinguished from the genomically coded $\gamma 2^{77I}$. A powerful way of doing this is the genetic introduction of either a small peptide sequence (tag) with high antigenicity (immuno-tagging) or high affinity to small molecules (affinity tagging) or reporter proteins with fluorescent properties (Kittler *et al.* 2000; Terpe, 2003; Giepmans *et al.* 2006). However, the tagging entails potential problems; the most obvious one is that the introduced tag itself affects the function and/or subcellular location of the target protein (Previtali *et al.* 2000; Limon *et al.* 2007).

First, we aimed to develop a widely applicable method for the efficient generation and testing of multiple tags and tag insertion sites. To facilitate the insertion of different affinity tags into different positions on the target protein we developed a DNA insertion method based on the work of Tomic *et al.* (1990). Our method combines the unrestricted freedom of choice of insertion positions used in the PCR-based mutagenesis techniques with the robustness and accuracy of directional ligation at restriction endonuclease (RE)-generated overhanging DNA ends. Type IIs REs (Szybalski *et al.* 1991) generate protruding DNA termini that differ from their recognition sequence by cutting at a defined distance from their recognition sites. A replaceable insert can be inserted into any position on a plasmid by inverse PCR (Ochman *et al.* 1988) and the insert can be completely removed later by a type IIs RE if the recognition sequence of the enzyme is present on the insert. The enzymatic cleavage leaves behind a at the insertion point surrounded by single-stranded regions of different lengths, determined by the type of the IIs RE used. The generated single-stranded ends can be used for ligation with synthetic oligo-nucleotides, holding complementary ends (Fig. 1).

We inserted five immuno- (Flag, 3XFlag (3XF), StrepII (SII), haemagglutinin (HA), and AU1) and one chemo-affinity (α-bungarotoxin binding site; BBS) tags between the 4th and 5th amino acid residues (referred to as N-terminal insertion) and at the C-terminus of the mature $GABA_AR$ $\gamma 2$ subunit. The tagged $\gamma 2$ subunit genes were used to replace the GFP gene in the pFUGW (Lois *et al.* 2002) lentiviral plasmid for generating lentiviral particles. Once lentiviruses containing N- and

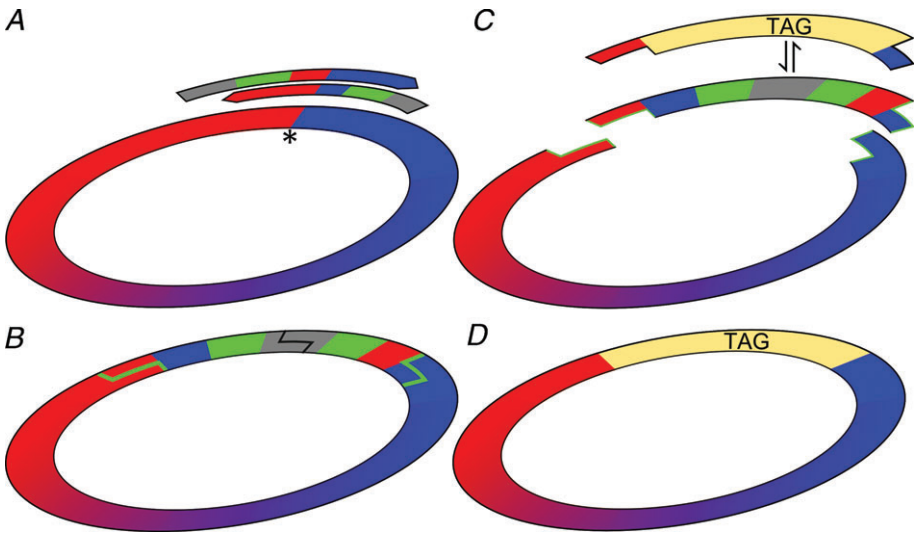

Figure 1. Site-independent insertion of epitope tags into the $GABA_A$ receptor $\gamma 2$ subunit cDNA
A, partially overlapping PCR primers with non-complementary 5′ tails coding for RE recognition sequences were designed to match the insertion point (*). *B*, both ends of the resulting PCR product were digested with EcoRI (grey) prior to self-circularization by T4-ligase. *C*, the sequence of the new plasmid was confirmed and then digested with BpII (green) which cuts outside of its recognition sequence (green lines), releasing the complete original plasmid sequence with protruding free ends. *D*, different tags, coded by double-stranded oligonucleotides with complementary protruding ends, were ligated in place of the removed insert. The recombinant tag-containing plasmids were selected by EcoRI digestion prior to transformation.

C-terminal-tagged $\gamma 2$ subunits were generated, we focused on the following questions. How efficiently can the tagged $\gamma 2$ subunits be detected? Does tagging affect the precise subcellular location of the subunit? Does tagging alter the kinetic and pharmacological properties of the receptors? To address these questions, we have applied light microscopic (LM) immunofluorescent reactions and patch-clamp electrophysiology in embryonic cortical cultures of control and $GABA_AR$ $\gamma 2^{-/-}$ mice and performed LM immunofluorescent and electron microscopic freeze-fracture replica immunogold labelling of the tagged $\gamma 2$ subunit and *in vitro* patch-clamp electrophysiology on brain slices of $GABA_AR\gamma 2^{77I}$lox mice.

Rescue of synaptic $GABA_A$Rs with lentiviral transduction of wild-type $\gamma 2$ subunits in $\gamma 2^{-/-}$ cultured cortical cells

Viral transduction of wild-type neurons with tagged $\gamma 2$ subunits has the disadvantage that the introduced subunit has to compete with the wild-type $\gamma 2$ subunit naturally expressed by the cells. Such a competition could result in unforeseen alterations in the assembly, trafficking and localization of the tagged subunit. Furthermore, the tagged subunit might be incorporated only into a small fraction of the receptors, precluding its efficient detection and functional scrutiny. To overcome this difficulty, we carried out viral transduction of neurons in which the endogenous $\gamma 2$ subunit is knocked out ($\gamma 2^{-/-}$; Günther *et al.* 1995). Unfortunately such deletion is lethal; therefore we were restricted to the use of primary neuronal cultures generated from $\gamma 2^{-/-}$ mice at embryonic day 16. First we used an anti-$\gamma 2$ and an anti-$\beta 2/3$ subunit antibody to determine the detectability and subcellular distribution of these subunits in $\gamma 2^{+/+}$ cultures ($\sim$21 DIV). As shown in Fig. 2*A*, our antibodies revealed a diffuse labelling throughout the somato-dendritic compartments of the cultured neurons with many strong immunoreactive clusters similar to that reported previously (Craig *et al.* 1994; Essricht *et al.* 1998). Next, we assessed the distribution of these subunits in cultured cells

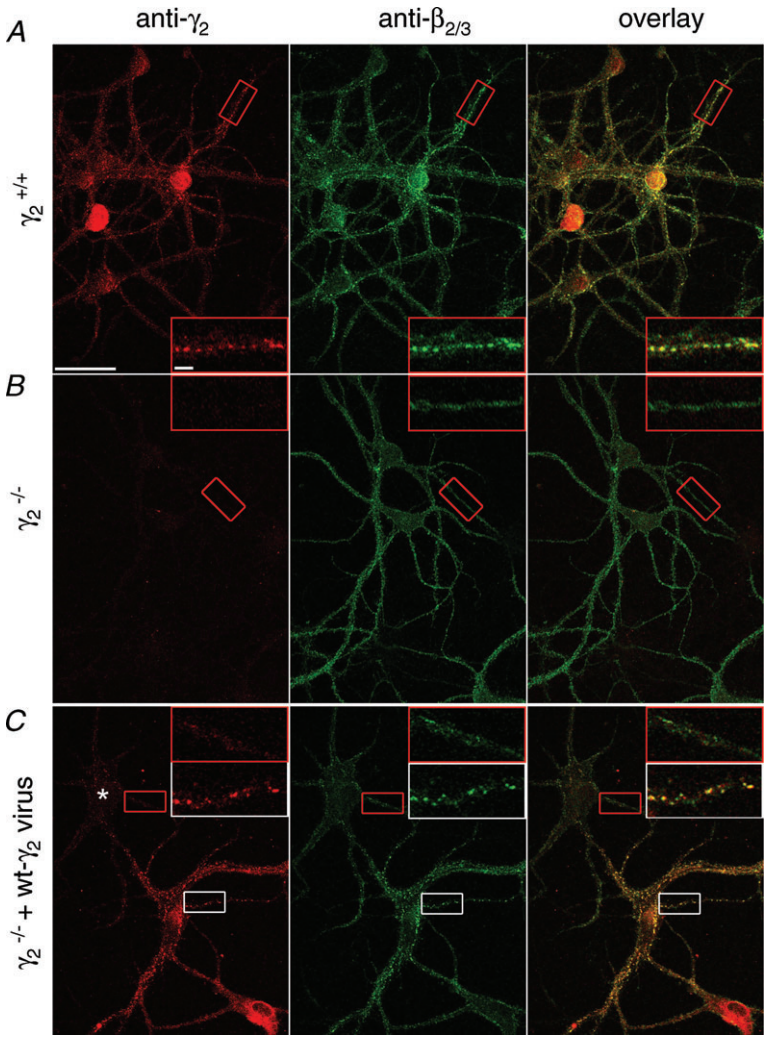

Figure 2. $GABA_A$ receptor clustering is rescued in $\gamma 2^{-/-}$ cultures following lentiviral introduction of wild-type $\gamma 2$ subunit
A–C, immunolocalization of the $\gamma 2$ and $\beta 2/3$ subunits in primary neuronal cell cultures derived from wild-type ($\gamma 2^{+/+}$; *A*), knock out ($\gamma 2^{-/-}$; *B* and *C*) cultures without (*A* and *B*) and following infection with wild-type $\gamma 2$-expressing lentiviruses (*C*). *A*, the $\gamma 2$ and $\beta 2/3$ subunits colocalize and form dendritic clusters in cultured neurons. *B*, in $\gamma 2^{-/-}$ cultures, immunolabelling for the $\gamma 2$ subunit completely disappears, whereas that for the $\beta 2/3$ subunits became diffuse, without forming dendritic clusters. *C*, a subset of cells in $\gamma 2^{-/-}$ cultures are infected with wild-type $\gamma 2$ subunit-expressing lentivirus and show intense punctate labelling for both the $\gamma 2$ and $\beta 2/3$ subunits. Note that $\beta 2/3$ labelling remained diffuse in an uninfected cell (asterisk). Boxed regions are enlarged in insets. Scale bars: main panels: 50 μm; insets: 5 μm.

obtained from $\gamma2^{-/-}$ mice (Fig. 2*B*). Immunolabelling for the $\gamma2$ subunit completely disappeared in these cells, demonstrating both the lack of $\gamma2$ subunit proteins as well as the specificity of our anti-$\gamma2$ labelling. A dramatic change in the distribution of $\beta2/3$ subunits was also observed similar to that reported earlier for another $GABA_A$R subunit ($\alpha2$; Essricht *et al.* 1998). The diffuse, non-clustered distribution of the β subunits is consistent with the essential role of the $\gamma2$ subunit for the synaptic clustering of the receptors. Next, we asked whether the lack of synaptic enrichment of the $GABA_A$Rs could be rescued by viral transduction of the $\gamma2^{-/-}$ cells with the $\gamma2^{77F}$ subunit. Application of viruses to the cultured cells resulted in a partial and random transduction among the cells; some cells showed strong immunoreactivity for the $\gamma2$ subunit, whereas others were just as negative as $\gamma2^{-/-}$ cells in non-transduced dishes (Fig. 2*C*). The immuno-positive cells showed a prominent clustering of both the $\gamma2$ and the $\beta2/3$ subunits, similar to that seen in $\gamma2^{+/+}$ cells. In summary, these experiments demonstrate that the lentiviral transduction of $\gamma2^{-/-}$ cells with the wild-type $\gamma2$ subunit can rescue the synaptic distribution of $\gamma2$ and $\beta2/3$ subunits.

Detectability and subcellular distribution of tagged $GABA_A$R $\gamma2$ subunits

Once the rescue of synaptic clustering of $GABA_A$Rs by the viral introduction of $\gamma2$ subunits was verified, we turned to the six N- and six C-terminal-tagged $\gamma2$ subunit-containing lentiviral constructs and tested the detectability and the subcellular distribution of the tagged subunits in $\gamma2^{-/-}$ cultured cells. As a general strategy, we used double immunofluorescent labelling with anti-$\gamma2$ and anti-tag antibodies. Strong, mainly cyto-plasmic immunosignal for the $\gamma2$ subunit was detected in most transduced cells irrespective of the tag and tagging location (cf. left panels on Fig. 3 and Supplemental Figs 1 and 2 (available online only)). In spite of this, the detection of the different tags showed enormous variability. For example, the Flag and BBS visualization resulted in the weakest signal and this was insertion site independent (Supplemental Figs 1 and 2). The N-terminal insertion of SII gave a weaker signal than the same tag at the C-terminal position (Supplemental Fig. 1), whereas for the AU1 tag the N-terminal tagging position resulted in a much stronger immunolabelling than the same tag at the C-terminal position (cf. Fig. 3*B* and Supplemental Fig. 2).

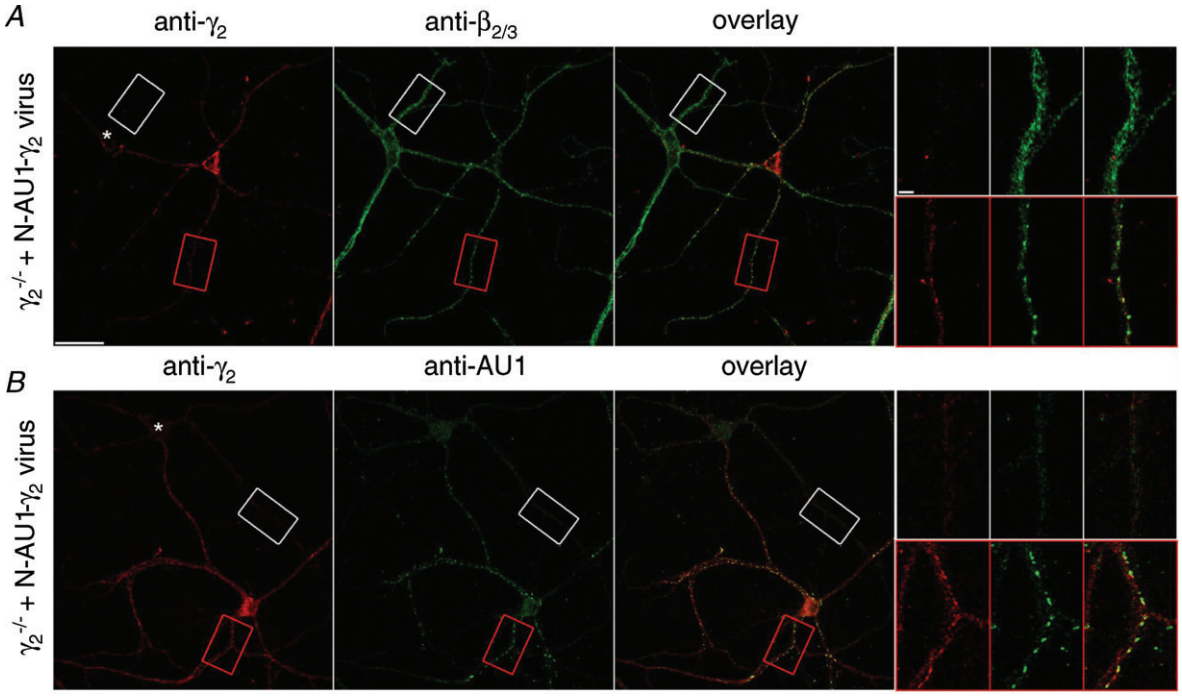

Figure 3. Tagging the $\gamma2$ subunit with the AU1 tag at an N-terminal position does not alter its subcellular distribution, but allows its efficient detection
Cultured $\gamma2^{-/-}$ cortical neurons were infected with $^{AU1}\gamma2^{77F}$ subunit- expressing lentivirus. Infected cells were double immunolabelled with either anti-$\gamma2$ and anti-$\beta2/3$ subunit antibodies (*A*) or anti-$\gamma2$ and anti-AU1 antibodies (*B*). Higher magnification views of dendrites from the boxed areas are shown in the insets. Immunoreactive clusters for the $\gamma2$ and $\beta2/3$ subunits colocalize in the infected dendrites (red boxes), but not in the uninfected cells (asterisk, white boxes). Note the very strong and punctate labelling obtained with the anti-AU1 antibody. Scale bars, main panels: 50 μm; insets: 5 μm.

The HA (Supplemental Fig. 2) and 3XF (Supplemental Fig. 1) tags could be visualized with relatively high efficiency, but the pattern of the labelling was different from that seen for the $\gamma 2$ subunit in wild-type cultures and in $\gamma 2^{-/-}$ cultures transduced with $\gamma 2$ subunits. A uniform and strong intracellular labelling was observed rather than clear synaptic plasma membrane clustering of the receptors, indicating that the insertion of these tags could have changed the subcellular distribution of the tagged $\gamma 2$ subunits. Out of the 12 different conditions, only the N-terminal AU1-tagged $\gamma 2$ subunit ($^{AU1}\gamma 2^{77F}$) provided a subcellular labelling pattern similar to that found in wild-type cultures. A clustered immunolabelling pattern was obtained with an anti-$\gamma 2$ subunit antibody, which showed an almost perfect co-localization with the $\beta 2/3$ subunits (Fig. 3*A*). The immunosignal obtained with the anti-AU1 antibody possessed a very high signal compared to the noise, consistent with the results of a previous study (Shevtsova *et al.* 2006). The images were dominated by clear, very intense synaptic clusters and low intensity extrasynaptic dendritic labelling (Fig. 3*B*).

Unaltered kinetic and pharmacological properties of AU1-tagged $\gamma 2$ subunits in cultures

The amplitude, rise and decay kinetics of IPSCs depend on the number, density and kinetic properties of post-synaptic $GABA_A$Rs and on the spatio-temporal profile of GABA in the synaptic cleft. Thus, the detailed analysis of the amplitude and kinetics of $GABA_A$R-mediated IPSCs is an excellent tool to deduce these properties of the receptors. In the next set of experiments, we carried out whole-cell voltage-clamp recordings of IPSCs evoked by spontaneous vesicular release of GABA. In the presence of a voltage-gated Na^+ channel blocker (0.5 μM TTX), NMDA (50 μM AP5) and non-NMDA (5 μM CNQX) receptor antagonists, spontaneously occurring inward currents were recorded from wild-type cultured cortical cells (Fig. 4*A*). A high Cl^--containing intracellular solution facilitated the detection of mIPSCs and resulted in inward current when recorded at –68 mV. The currents had fast rise times and exponential decays and an average amplitude of 54.1 ± 7.7 pA. In $\gamma 2^{-/-}$ cells, mIPSCs could be readily detected (Fig. 4*B*), in agreement with a previous study (Essricht *et al.* 1998), and had a similar rise time, peak amplitude, but a significantly slower decay time (35.7 ± 3.8 ms *vs.* 16.6 ± 0.9 ms) compared to $\gamma 2^{+/+}$ cells (Fig. 4*B* and *F*). When the $\gamma 2^{-/-}$ cells were transduced with either wild-type $\gamma 2$ (Fig. 4*C*) or $^{AU1}\gamma 2^{77F}$ (Fig. 4*D*) subunits, the amplitude and kinetics of mIPSCs were fully rescued and were indistinguishable from those recorded from control cells. Because the $\gamma 2$ subunit confers BZ sensitivity to most $GABA_A$Rs, we applied 1 μM zolpidem, a BZ site agonist, and examined its effect on the amplitude and kinetics of the mIPSCs. As shown in Fig. 4*E*, zolpidem increased the amplitude and prolonged the decay of mIPSCs in control cells, but had no effect on $\gamma 2^{-/-}$ mIPSCs, consistent with the lack of $\gamma 2$ subunits and its essential role in conferring BZ sensitivity. The effect of zolpidem on mIPSC amplitudes and decays was fully rescued by the viral introduction of $\gamma 2^{77F}$ or $^{AU1}\gamma 2^{77F}$ subunits. In summary, our physiological and pharmacological experiments demonstrate the lack of unwanted effects following insertion of the AU1 tag into the N-terminal region of the $\gamma 2$ subunit.

Cre-recombinase-mediated removal of $GABA_A$R $\gamma 2$ subunits from $GABA_A R\gamma 2^{77I}$lox cortical cells

Next, we carried out *in vivo* experiments to remove the $GABA_A$R $\gamma 2$ subunits from cortical cells. By transducing neocortical pyramidal cells of $GABA_A R\gamma 2^{77I}$lox mice following stereotaxic injection of Cre-recombinase-containing lentiviruses we tested the subcellular distribution of $GABA_A$R subunits. Figure 5*A* demonstrates that the local injection of Cre-recombinase-containing lentiviruses into the neocortex results in a large reduction in the immunolabelling for the $\gamma 2$ subunit. A similar injection into the contralateral side with lentiviruses expressing eGFP caused no change in the $\gamma 2$ immunofluorescent labelling. Examining the LM immunofluorescent reaction at high magnifications revealed that the $\gamma 2$ subunit was missing only from the Cre-expressing neurons (Fig. 5*B*). In these cells, perisomatic plasma membranes were completely devoid of $\gamma 2$ subunit immunolabelling. To verify further the lack of synaptic labelling of the $\gamma 2$ subunit, we performed SDS-digested freeze-fracture replica labelling (SDS-FRL) (Fujimoto, 1995; Masugi-Tokita & Shigemoto, 2007; Lorincz & Nusser, 2010) on cortical tissue obtained from the injection sites. Because SDS treatment in this method washes away all the soluble proteins, we were unable to detect the virally introduced Cre-recombinase. We knew from the LM immunofluorescent reactions, however, that not all, but only a fraction of the cells were virally transduced in the middle of the injection area. Thus, we predicted that by examining a large number of cell bodies within the injection area at the electron microscopic level, we would randomly encounter Cre-negative as well as Cre-positive cells. Indeed, we found the exoplasmic plasma membrane faces (E-faces) of cell bodies without any (Fig. 5*D*) and with many $\gamma 2$ (Fig. 5*F*) immunopositive synapses. Since our anti-$\gamma 2$ antibody reacts with extracellular epitopes of the subunit, labelling for the $\gamma 2$ subunit appears on the E-face, which lacks clear structural features for demarcating GABAergic synapses (Kasugai *et al.* 2010). In order to unequivocally identify the GABAergic synapses on E-face structures,

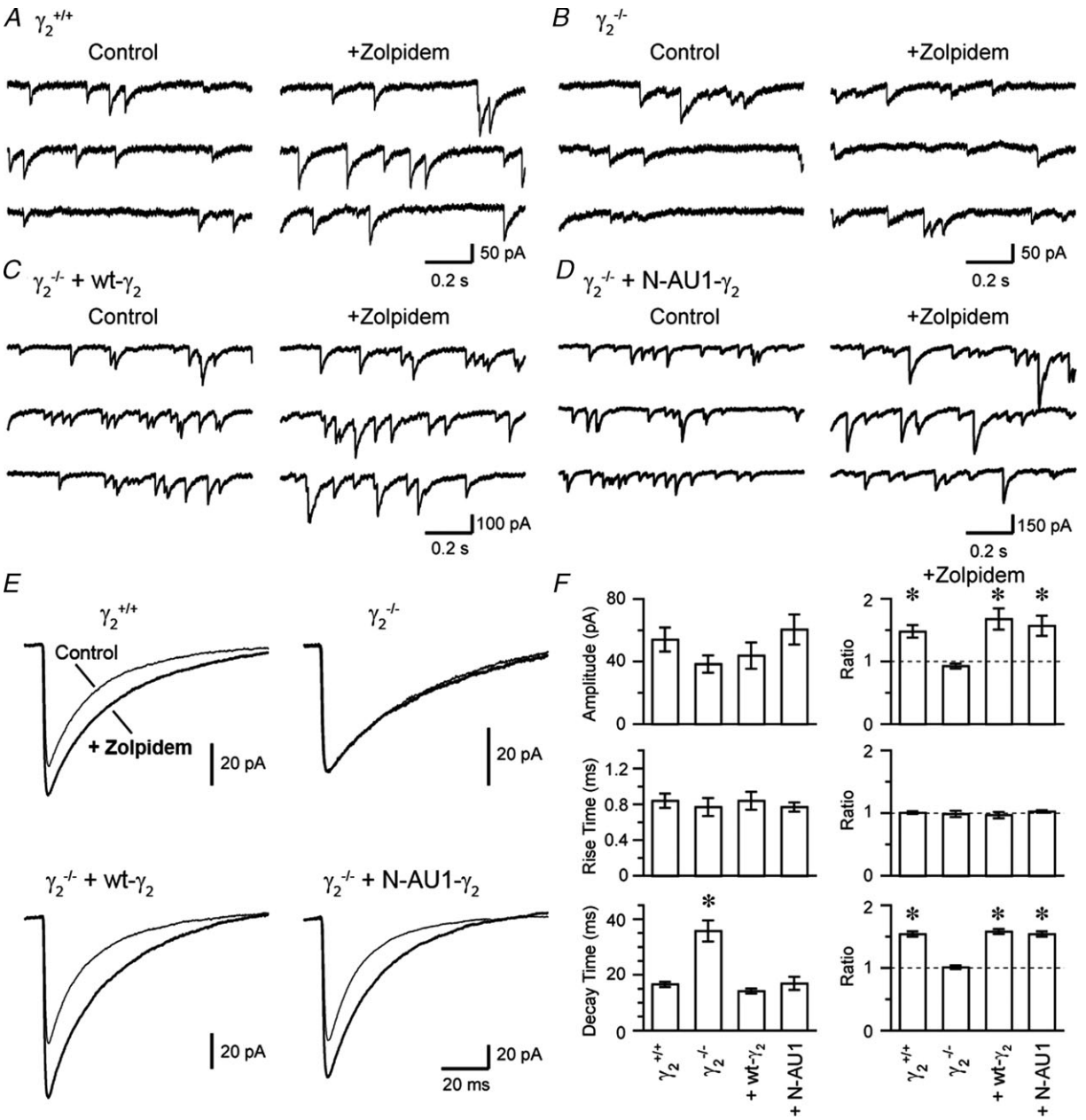

Figure 4. Electrophysiological verification of the unaltered properties of the N-terminal AU1-tagged $\gamma 2$ subunits

A–D, continuous 3 s whole-cell voltage-clamp recordings are shown from $\gamma 2^{+/+}$ (*A*), $\gamma 2^{-/-}$ (*B*), $\gamma 2^{-/-}$ + $\gamma 2^{77F}$ (*C*) and $\gamma 2^{-/-}$ + $^{AU1}\gamma 2^{77F}$ (*D*) cortical cultured neurons in the presence of 0.5 μM TTX, 5 μM CNQX and 50 μM AP5 (Control) and after addition of 1 μM zolpidem (+Zolpidem). *E*, superimposed averaged mIPSCs are shown in the presence and absence of zolpidem in $\gamma 2^{+/+}$ (top left), $\gamma 2^{-/-}$ (top right) cultures without viral transduction and in $\gamma 2^{-/-}$ cultures transduced with wild-type $\gamma 2$ subunit (bottom left) and $\gamma 2^{-/-}$ cultures transduced with $^{AU1}\gamma 2^{77F}$ subunit (bottom right). *F*, summary of the kinetics and the effect of zolpidem on GABAergic mIPSCs recorded under different conditions. The ratios of the amplitude, the rise time and the decay time before and after zolpidem application are shown on the right. Compared to mIPSCs recorded in $\gamma 2^{+/+}$ cultured cells, mIPSCs in $\gamma 2^{-/-}$ cultured cells had similar amplitudes and rise times, but had ~2 times longer decay times. In addition, zolpidem affected the amplitude and the decay time of the wild-type mIPSCs, but was ineffective in modulating $\gamma 2^{-/-}$ mIPSCs. The kinetic properties and the benzodiazepine sensitivity of the $\gamma 2^{-/-}$ cultures are restored following the lentiviral transduction with the $\gamma 2^{77F}$ subunit and the $^{AU1}\gamma 2^{77F}$ subunit. The * on the left columns indicates significant differences ($P < 0.05$) using ANOVA and Fisher's PLSD *post hoc* test and the * on the right column indicates significant difference ($P < 0.05$) from control following zolpidem application using a paired *t* test.

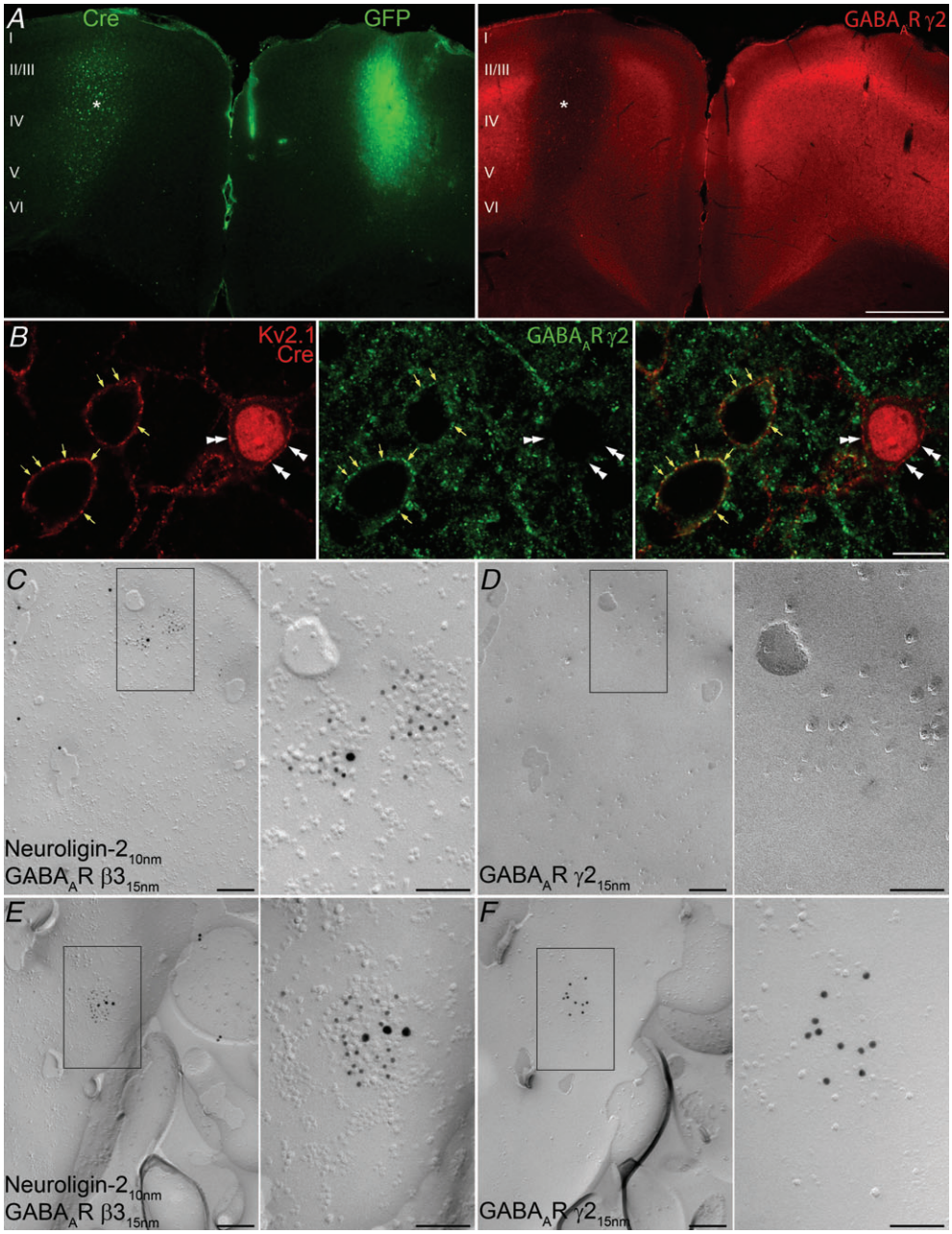

Figure 5. *In vivo* lentiviral expression of Cre-recombinase disrupts the expression of the GABA$_A$R γ2 subunit in neocortical neurons of GABA$_A$Rγ2^{77I}lox mice

A, double immunofluorescent reaction reveals the absence of GABA$_A$R γ2 immunoreactivity (right panel, asterisk) in the neocortex expressing Cre-recombinase (left panel, asterisk), whereas immunoreactivity for the γ2 subunit is not altered in the contralateral neocortex transduced with eGFP, which was detected by its fluorescence. *B*, punctate immunolabelling for the γ2 subunit is associated with the plasma membrane (yellow arrows) of non-transduced, control neocortical neurons outlined by a Kv2.1 subunit immunolabelling, but is not present in the plasma membrane (double arrowheads) of a Cre-recombinase-expressing neuron. *C* and *D*, P- (*C*) and E-faces (*D*) of the same somatic plasma membrane of a transduced cell are shown using the 'mirror replica technique'. Enlarged views of the boxed areas in *C* and *D* are shown on the right. Immunogold particles labelling neuroligin-2 (10 nm gold) and GABA$_A$R β3 (15 nm gold) are accumulated over the postsynaptic membrane of a GABAergic synapse marked by the loose cluster of intramembrane particles, whereas immmunogold labelling for the GABA$_A$R γ2 (15 nm gold) subunit is absent from the corresponding E-face of the same postsynaptic membrane. *E* and *F*, P- (*E*) and E-faces (*F*) of the somatic plasma membrane of a control, non-transduced cell body are shown using the 'mirror replica technique'. Immmunogold particles for the γ2 subunit (15 nm gold) are concentrated in the E-face of the postsynaptic membrane, also labelled for neuroligin-2 (10 nm gold) and GABA$_A$R β3 (15 nm gold) on the corresponding P-face. Scale bars: 500 μm (*A*); 10 μm (*B*); 200 nm (*C*, *D*, *E* and *F*); 100 nm (insets).

all experiments were performed with the 'mirror replica method' (Hagiwara *et al.* 2005). With this method, replicas are generated from both matching sides of the fractured tissue surfaces, allowing the examination of the corresponding E-faces and protoplasmic or P-faces of exactly the same membranes. On the P-face, immunolabelling for neuroligin-2 and $GABA_AR$ $\beta3$ subunit (Fig. 5C and E) together with clusters of intramembrane particles clearly demarcated GABAergic synapses (Kasugai *et al.* 2010), allowing the direct examination of the same synapses on the corresponding E-face with respect to their immunoreactivity for the $\gamma2$ subunit. On cell bodies that contained $\gamma2$ subunit-immunopositive GABAergic synapses, all examined synapses were immunopositive for the $\gamma2$ subunit. In contrast, if a soma had synapses that were immunonegative for the $\gamma2$ subunit, all of its synapses were immunonegative. These results provide compelling evidence for the total lack of $GABA_AR$ $\gamma2$ subunits in the perisomatic GABAergic postsynaptic plasma membranes of neocortical neurons following viral transduction with Cre-recombinase.

Efficient detectability, unaltered synaptic localization and kinetic properties of the AU1-tagged $\gamma2$ subunit-containing $GABA_ARs$

Next, we tested the detectability and subcellular distribution of virally introduced AU1-tagged $GABA_AR$ $\gamma2$ subunits *in vivo*. For this, we generated lenti- and adeno-associated viruses containing Cre-recombinase and $^{AU1}\gamma2^{77F}$, separated by a 2A-peptide-like sequence (Donnelly *et al.* 2001; Cre-2A-$^{AU1}\gamma2^{77F}$). Following the stereotaxic injection of these viruses into the neocortex of $GABA_AR\gamma2^{77I}$lox mice, LM immunofluorescent reactions demonstrated the strong expression of Cre-recombinase and AU1 around the injection site (Fig. 6*A*). The plasma membranes of all neurons with nuclear labelling for Cre-recombinase were strongly decorated by intense, punctate immunofluorescent labelling for AU1 (Fig. 6*B*). Such AU1 clusters co-localized with the GABAergic synapse marker gephyrin (Fig. 6*C*), indicating that the AU1-tagged $\gamma2$ subunits took up proper synaptic locations. For a direct demonstration of this, we carried out SDS-FRL in the injection area and immunolabelled mirror replicas with neuroligin-2 and the $GABA_AR$ $\beta3$ subunit on P-faces (Fig. 6*D* and *F*) and the $\gamma2$ subunit and AU1 on the corresponding E-faces (Fig. 6*E* and *G*). Somatic plasma membranes of all neurons contained large numbers of neuroligin-2- and $\beta3$-immunopositive synapses (Fig. 6*D* and *F*), which were all immunopositive for the $\gamma2$ subunit as well. Only some of the cells contained synapses that were labelled for AU1 (Fig. 6*E*). However, all synapses in such cells contained a large number of gold particles labelling the AU1 epitope, demonstrating a high efficiency of the AU1 immunodetection using SDS-FRL and correct synaptic targeting of the AU1-tagged $\gamma2$ subunit.

In our final sets of experiments, we performed whole-cell voltage-clamp recordings from acute cortical slices 2–7 weeks after the injection of Cre-2A-$^{AU1}\gamma2^{77F}$ lenti- and adeno-associated viruses. In all cells, fast rising, exponentially decaying spontaneous inward currents were recorded in the presence of TTX (1 μM) and kynurenic acid (3 mM; Fig. 7*A* and *B*), which were blocked by the $GABA_AR$ antagonist SR95531. When the recorded cells were grouped based on their immunonegativity or positivity for Cre-recombinase determined *post hoc*, there was no significant difference in the frequency (3.6 ± 2.4 Hz, $n = 8$ Cre– cells *vs.* 4.1 ± 2.7 Hz, $n = 5$ Cre+ cells), amplitude (11.2 ± 3.0 pA *vs.* 11.1 ± 4.0 pA), 10–90% rise time (0.49 ± 0.11 ms *vs.* 0.55 ± 0.13 ms) and weighted decay time constant (τ_w; 6.3 ± 2.3 ms *vs.* 6.7 ± 0.8 ms) of mIPSCs between the two cell populations (Fig. 7*C*). However, when the effect of 1 μM zolpidem was tested on the decay of mIPSCs, there was no significant change ($P = 0.25$, paired t test) in Cre-negative cells (before drug: 6.3 ± 2.3 ms *vs.* drug: 7.3 ± 4.0 ms), but a significant ($P < 0.05$, paired t test) slowing of the decay was observed in Cre-positive cells (before drug: 6.7 ± 0.8 ms *vs.* drug: 11.8 ± 2.8 ms). We then specifically investigated the restoration of zolpidem sensitivity of the perisomatic synaptic receptors activated by fast spiking GABAergic basket cells. For this, we performed double whole-cell recordings in the absence of TTX from a presynaptic fast-spiking basket cell and a postsynaptic pyramidal cell (PC; Fig. 7*D*). Brief depolarizing current injections into the presynaptic cell reliably evoked fast rising, exponentially decaying IPSCs, the decay of which was prolonged by 1 μM zolpidem (Fig. 7*E*). *Post hoc* analysis of the recorded cells revealed that the postsynaptic PC was immunopositive for Cre-recombinase (Fig. 7*F*). These results demonstrate the unaltered synaptic localization of $GABA_ARs$ and similar kinetics of postsynaptic currents following viral swapping of $\gamma2^{77I}$ with $^{AU1}\gamma2^{77F}$, and the restoration of zolpidem sensitivity of the synaptic currents.

Discussion

In the present work, we have developed a fast, efficient cloning strategy for site-independent insertion of different immuno- and affinity tags to target proteins. First, we have examined six N- and six C-terminal-tagged $GABA_AR$ $\gamma2$ subunits and found that only a single construct fulfilled all the requirements; namely high detection efficiency, genuine wild-type-like subcellular distribution and the rescue of mIPSCs in $\gamma2^{-/-}$ cultures, while conferring normal amplitude, kinetics and BZ

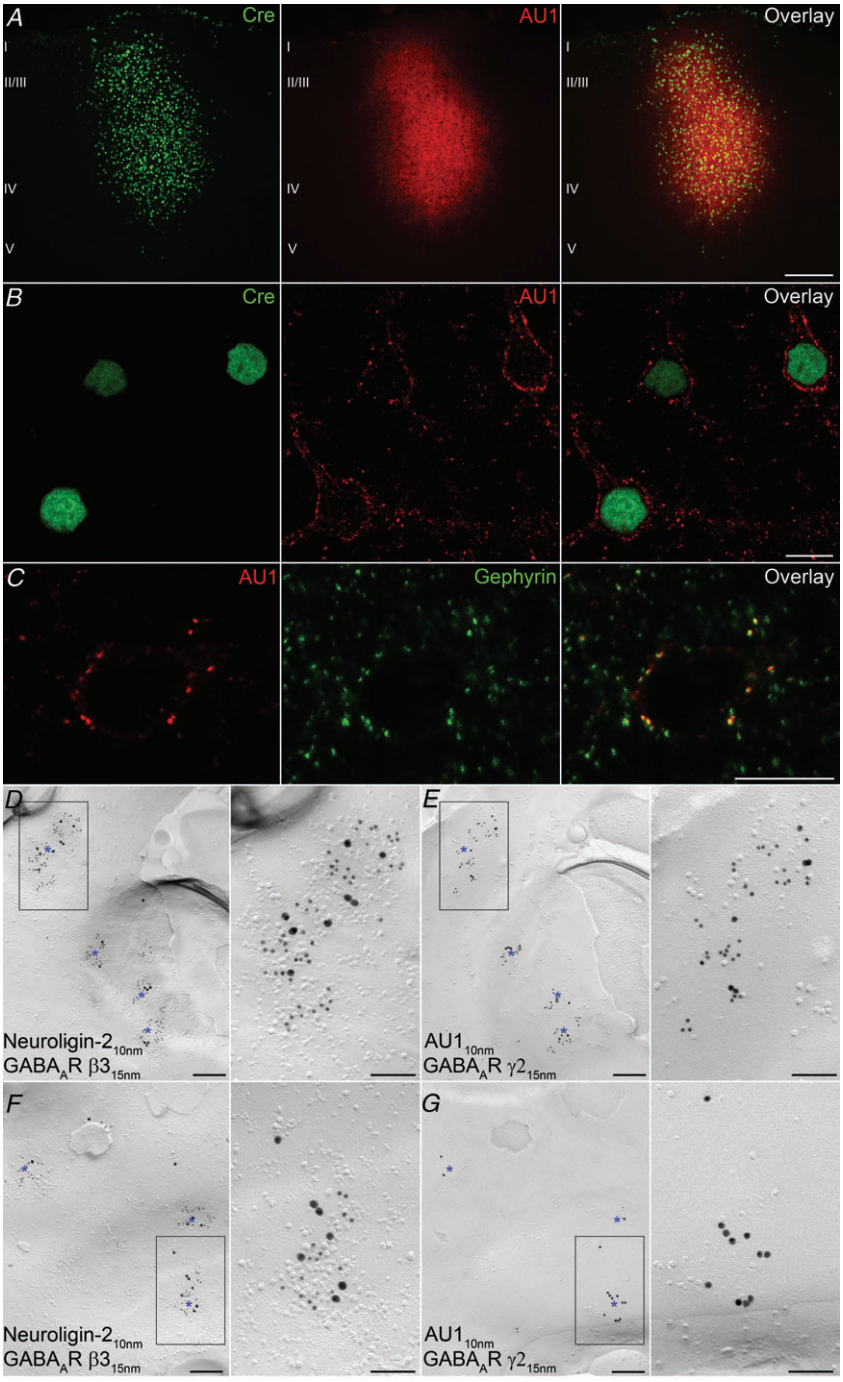

Figure 6. *In vivo* lentiviral replacement of $\gamma 2^{77I}$ with $^{AU1}\gamma^{277F}$ in neocortical neurons
A, double immunofluorescent reactions demonstrate the co-expression of Cre-recombinase and AU1 in neocortical neurons transduced with a lentivirus containing Cre-2A-$^{AU1}\gamma 2^{77F}$. *B*, higher magnification view showing the nuclear expression of Cre-recombinase and plasma membrane-associated AU1 labelling in the transduced neurons. *C*, co-localization of AU1 and gephyrin in the perisomatic synapses of a transduced neuron. *D* and *E*, P- (*D*) and E-faces (*E*) of a somatic plasma membrane of a transduced cell are shown using the 'mirror replica technique'. Higher magnification images of the boxed areas are shown on the right. Immunogold particles for the AU1 (10 nm gold) and $GABA_AR$ $\gamma 2$ subunit (15 nm gold) are concentrated in the E-face of the postsynaptic membrane also labelled for neuroligin-2 (10 nm gold) and $GABA_AR$ $\beta 3$ (15 nm gold) on the corresponding P-face. *F* and *G*, P- (*F*) and E-faces (*G*) of a somatic plasma membrane of a non-transduced cell are shown using the 'mirror replica technique'. Immunogold particles for the $\gamma 2$ subunit (15 nm gold), but not that of the AU1 (10 nm gold) are concentrated in the E-face of the postsynaptic membrane. The same synapses are also labelled for neuroligin-2 (10 nm gold) and $\beta 3$ subunit (15 nm gold) on the corresponding P-face. Asterisks indicate GABAergic synapses. Scale bars: 200 μm (*A*); 10 μm (*B* and *C*); 200 nm (*D*, *E*, *F* and *G*); 100 nm (insets).

pharmacology to the $GABA_A$Rs. We then generated both lenti- and adeno-associated viruses, which contained both the Cre-recombinase and the N-terminal AU1-tagged wild-type $\gamma 2$ subunit, separated by a 2A-peptide-like sequence. These viruses allowed the brain region-specific swapping of $\gamma 2^{77I}$ with $^{AU1}\gamma 2^{77F}$. The resulting $GABA_A$Rs had normal synaptic enrichment, unaltered kinetic properties and restored sensitivity to zolpidem.

Most of the recently developed pharmacogenetic approaches rely on the genetic introduction of an exogenous protein to the targeted mammalian neuron. This is true for the *Drosophila* allatostatin receptor (Lechner *et al.* 2002; Tan *et al.* 2006), the *C. elegans* ivermectin-sensitive Cl^- channels (Slimko *et al.* 2002), the mutated human muscarinic receptor (Armbruster *et al.* 2007; Ferguson *et al.* 2011) and the $\alpha 7$ nicotinic and glycine

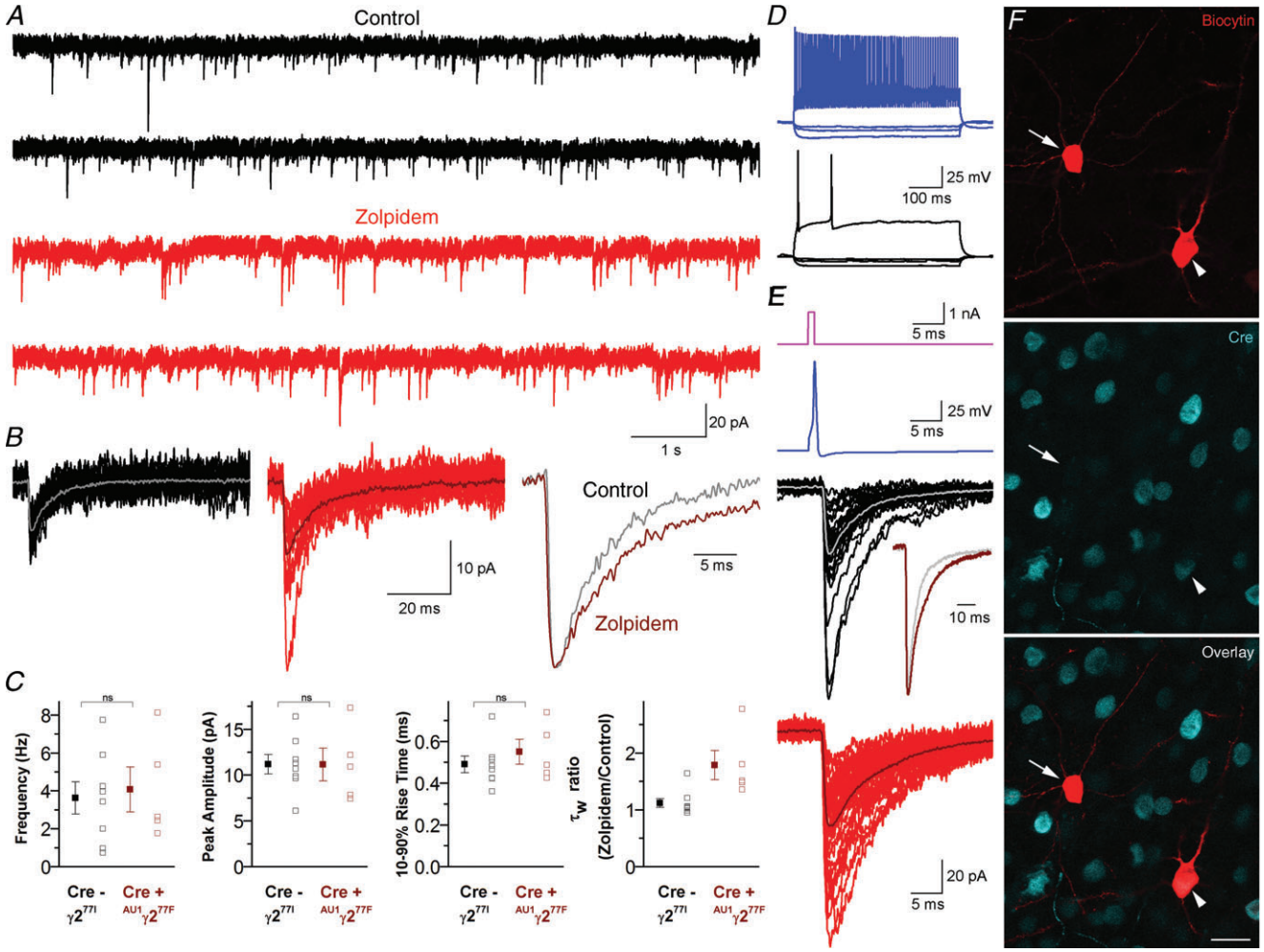

Figure 7. Virus-mediated replacement of $\gamma 2^{77I}$ with $^{AU1}\gamma 2^{77F}$ restores IPSC sensitivity to zolpidem in Cre-immunopositive layer 2/3 pyramidal cells
A, continuous current recordings from a Cre-positive layer 2/3 pyramidal cell in ACSF (upper, black) and 1 μM zolpidem (lower, red). *B*, superimposed consecutive mIPSCs in control (left, black, average in grey) and 1 μM zolpidem (centre, red, average in dark red) from the cell shown in *A*. Peak-scaled, peak-aligned average traces are shown on the right. *C*, plots of the population mean ± SEM and individual cell mean values of mIPSC frequency, peak amplitude, 10–90% rise time and the weighted decay time constant (τ_w) ratio (zolpidem/control) from 8 Cre-negative (grey) and 5 Cre-positive (dark red) cells. *D*, voltage responses of a fast-spiking basket cell (upper, blue) and a layer 2/3 pyramidal cell (lower, black) to 500 ms hyperpolarizing and depolarizing current injections. *E*, brief current pulses (top, magenta) were used to trigger single action potentials in the basket cell (upper, blue), evoking IPSCs in the simultaneously recorded pyramidal cell (lower, individual sweeps in black, average in grey). After wash in of 1 μM zolpidem (bottom, individual sweeps in red, average in dark red), peak amplitude and τ_w values were increased. The change in kinetics can be clearly seen from the superimposed peak-scaled, peak-aligned average traces (inset in lower panel). *F*, single confocal section showing *post hoc* visualization of biocytin (red) and immunofluorescent detection of Cre-recombinase (cyan) in the recorded basket cell (Cre-negative, arrow) and pyramidal cell (Cre-positive, arrowhead) shown in panels *D* and *E*. Scale bar: 20 μm.

receptor chimera (Magnus *et al.* 2011). The so-called 'designer receptor' approach holds great promise, allowing the selective increase or decrease in the activity of a well-defined neuronal population (Armbruster *et al.* 2007; Ferguson *et al.* 2011; Magnus *et al.* 2011). Here, the ligand-binding sites of known ligand-gated ion channels (e.g. α7 nicotinic) or G-protein-coupled receptors (e.g. human M4 muscarinic) are mutated in order to remove their sensitivity to their endogenous ligands and to confer sensitivity to small synthetic ligands that are otherwise pharmacologically inert. The introduction of such designer receptors either by creating transgenic animals or by using viral vectors makes the targeted cells selectively sensitive to pharmacological manipulations. The application of the appropriate drug activates these receptors, leading to either direct ion flux through the receptors or through G-protein-coupled inward-rectifying K^+ channels. There are two potential problems with these methods. One is the unforeseen effects of the genetically coded and mutated receptors on the assembly and subcellular targeting of the endogenous wild-type proteins. How the pentameric assembly of endogenous Gly or nicotinic receptors in the endoplasmic reticulum is affected by the transgenically introduced α7-GlyR is unknown. A potentially even more alarming issue is the partial activation of the mutated receptors with their original endogenous ligands or their unforeseen constitutive activity. These problems would lead to changes in the passive membrane properties and the excitability of the transduced cells in the absence of the designed ligands. As these genetic manipulations take place either throughout the whole life of the animal or over several weeks in the case of viral transduction, such long-standing alterations in the excitability of the target cell population could lead to unforeseen compensatory effects. The pharmacogenetic approach developed by Wulff *et al.* (2007) is the only available method that does not depend on the introduction of exogenous proteins into the target cell population, conferring a great advantage to this method. However, the generation of two additional mouse lines – one expressing Cre-recombinase and the other expressing the wild-type γ2 subunit – makes the original method of Wulff *et al.* (2007) cumbersome. Moreover, $\gamma2^{77F}$ subunit expression was driven by the L7 promoter, which may cause altered $GABA_A$R-mediated inhibition during development. Here we demonstrated the development of lenti- and adeno-associated virus-based swapping of mutated $\gamma2^{77I}$ with the AU1-tagged wild-type, zolpidem-sensitive γ2 subunit in cortical pyramidal cells. We also employed a large repertoire of anatomical and *in vitro* electrophysiological methods to verify the unaltered subcellular/synaptic distribution and unaltered kinetic properties of the virally introduced $^{AU1}\gamma2^{77F}$ subunit.

There is a general agreement that affinity tagging of proteins holds great promise (Giepmans *et al.* 2006), but could result in potential problems, the lack of which must be rigorously tested before the analysis of function with the tagged protein (Previtali *et al.* 2000; Limon *et al.* 2007). For ion channels, such functional tests are often confined to examining the ionic currents flowing through the channels when they are expressed in heterologous expression systems. It is now widely accepted that the function of ion channels is regulated by a large family of interacting proteins, which are only present in their natural subcellular environments (Ehlers *et al.* 1996; Moss & Smart, 2001; Trimmer & Rhodes, 2004). Thus, it seems rational to suggest that the functional verification of affinity tagging must be carried out in the natural environment of the protein. For most synaptic neurotransmitter receptors, this site is the postsynaptic density opposite to the presynaptic active zone where transmitter molecules are released. Thus the analysis of postsynaptic currents provides the best indication of any alteration of the receptor location, density, ligand-binding and gating properties. In addition, we believe that affinity-tagged proteins should be expressed in cells that do not express genomic, non-tagged copies of the same protein. A simple over-expression approach ends up with a competition between the tagged and non-tagged proteins, the result of which is highly unpredictable. The most foreseeable problem might be that only a small proportion of the proteins in a given location will be the tagged ones, and therefore their altered function might not be detected upon verification. For example, if tagged neurotransmitter receptors are expressed in nerve cells, which endogenously express the same receptor, a scenario might be envisaged whereby only a small fraction of the postsynaptically clustered receptors will be tagged, and therefore their altered conductance, kinetics or pharmacological properties will remain unnoticed when the synaptic currents are examined. This necessitates the use of either conventional knock-out animals/cultured cells or the endogenous gene might be deleted using the Cre-LoxP (or other similar recombination) system in only those cells where the tagged proteins are expressed. In the present study, we used virus-mediated expression of Cre and $\gamma2^{77F}$, which has a few advantages over the transgenic strategy used by Wulff *et al.* (2007). First, we can exclude unwanted alterations of the γ2 subunit expression during development that could affect neuronal circuit formation. Second, using multiple kinds of viruses carrying different promoters or elements of alternative conditional recombination systems, it will be possible to express $\gamma2^{77F}$ in multiple cell types of different brain regions.

In the present work, using combined light- and electron microscopic immunolocalizations and *in vitro* patch-clamp electrophysiology, we have provided a proof of principle for the generation of an immunotagged $GABA_A$R γ2 subunit that has unaltered subcellular

distribution, synaptic density and kinetic properties. In $\gamma2^{-/-}$ cortical cells, the lentiviral expression of wild-type $\gamma2$ subunits rescued the kinetic and pharmacological properties of mIPSCs and such physiological and pharmacological rescue was indistinguishable when $^{AU1}\gamma2^{77F}$ was used. Having established the lack of functional effects of N-terminal tagging of the $\gamma2$ subunit with the small immunotag AU1 in cultured cells, we turned to *in vivo* experiments to verify the proper subcellular/synaptic location and the detectability of the tagged receptors with an anti-AU1 antibody. Light microscopic immunofluorescent localization allowed the efficient and highly specific visualization of the $^{AU1}\gamma2^{77F}$ subunit in cortical cells following *in vivo* stereotaxic injection of lenti- or adeno-asociated viruses. Intense immunofluorescent puncta decorated the Cre-expressing cells without any detectable signal in the surrounding non-transduced cells. Not only was the detection efficiency of the AU1 tag remarkable, but also the extremely low non-specific labelling outside the injection zone. To our great delight, the AU1 tag was also detected very efficiently with the highly sensitive, high resolution SDS-FRL method, opening up new avenues for the applicability of AU1 immunotagging cell surface proteins, including neurotransmitter receptors and ion channels.

References

Armbruster BN, Li X, Pausch MH, Herlitze S & Roth BL (2007). Evolving the lock to fit the key to create a family of G protein-coupled receptors potently activated by an inert ligand. *Proc Natl Acad Sci U S A* **104**, 5163–5168.

Callaway EM (2005). A molecular and genetic arsenal for systems neuroscience. *Trends Neurosci* **28**, 196–201.

Craig AM, Blackstone CD, Huganir RL & Banker G (1994). Selective clustering of glutamate and γ-aminobutyric acid receptors opposite terminals releasing the corresponding neurotransmitters. *Proc Natl Acad Sci U S A* **91**, 12373–12377.

Donnelly ML, Hughes LE, Luke G, Mendoza H, ten Dam E, Gani D & Ryan MD (2001). The 'cleavage' activities of foot-and-mouth disease virus 2A site-directed mutants and naturally occurring '2A-like' sequences. *J Gen Virol* **82**, 1027–1041.

Ehlers MD, Mammen AL, Lau LF & Huganir RL (1996). Synaptic targeting of glutamate receptors. *Curr Opin Cell Biol* **8**, 484–489.

Essricht C, Lorez M, Benson JA, Fritschy J-M & Lüscher B (1998). Postsynaptic clustering of major $GABA_A$ receptor subtypes requires the $\gamma2$ subunit and gephyrin. *Nat Neurosci* **1**, 563–571.

Ferguson SM, Eskenazi D, Ishikawa M, Wanat MJ, Phillips PE, Dong Y, Roth BL & Neumaier JF (2011). Transient neuronal inhibition reveals opposing roles of indirect and direct pathways in sensitization. *Nat Neurosci* **14**, 22–24.

Fujimoto K (1995). Freeze-fracture replica electron microscopy combined with SDS digestion for cytochemical labelling of integral membrane proteins. Application to the immunogold labelling of intercellular junctional complexes. *J Cell Sci* **108**, 3443–3449.

Giepmans BN, Adams SR, Ellisman MH & Tsien RY (2006). The fluorescent toolbox for assessing protein location and function. *Science* **312**, 217–224.

Günther U, Benson J, Benke D, Fritschy JM, Reyes G, Knoflach F, Crestani F, Aguzzi A, Arigoni M, Lang Y, Bluethmann H, Mohler H & Lüscher B (1995). Benzodiazepine-insensitive mice generated by targeted disruption of the $\gamma2$ subunit gene of γ-aminobutyric acid type A receptors. *Proc Natl Acad Sci U S A* **92**, 7749–7753.

Hagiwara A, Fukazawa Y, Deguchi-Tawarada M, Ohtsuka T & Shigemoto R (2005). Differential distribution of release-related proteins in the hippocampal CA3 area as revealed by freeze-fracture replica labelling. *J Comp Neurol* **489**, 195–216.

Kasugai Y, Swinny JD, Roberts JD, Dalezios Y, Fukazawa Y, Sieghart W, Shigemoto R & Somogyi P (2010). Quantitative localisation of synaptic and extrasynaptic $GABA_A$ receptor subunits on hippocampal pyramidal cells by freeze-fracture replica immunolabelling. *Eur J Neurosci* **32**, 1868–1888.

Kittler JT, Wang J, Connolly CN, Vicini S, Smart TG & Moss SJ (2000). Analysis of $GABA_A$ receptor assembly in mammalian cell lines and hippocampal neurons using $\gamma2$ subunit green fluorescent protein chimeras. *Mol Cell Neurosci* **16**, 440–452.

Lechner HA, Lein ES & Callaway EM (2002). A genetic method for selective and quickly reversible silencing of mammalian neurons. *J Neurosci* **22**, 5287–5290.

Lerchner W, Xiao C, Nashmi R, Slimko EM, van Trigt L, Lester HA & Anderson DJ (2007). Reversible silencing of neuronal excitability in behaving mice by a genetically targeted, ivermectin-gated Cl^- channel. *Neuron* **54**, 35–49.

Limon A, Reyes-Ruiz JM, Eusebi F & Miledi R (2007). Properties of GluR3 receptors tagged with GFP at the amino or carboxyl terminus. *Proc Natl Acad Sci U S A* **104**, 15526–15530.

Lois C, Hong EJ, Pease S, Brown EJ & Baltimore D (2002). Germline transmission and tissue-specific expression of transgenes delivered by lentiviral vectors. *Science* **295**, 868–872.

Lorincz A & Nusser Z (2010). Molecular identity of dendritic voltage-gated sodium channels. *Science* **238**, 906–909.

McClive PJ & Sinclair AH (2001). Rapid DNA extraction and PCR-sexing of mouse embryos. *Mol Reprod Dev* **60**, 225–226.

Magnus CJ, Lee PH, Atasoy D, Su HH, Looger LL & Sternson SM (2011). Chemical and genetic engineering of selective ion channel-ligand interactions. *Science* **333**, 1292–1296.

Masugi-Tokita M & Shigemoto R (2007). High-resolution quantitative visualization of glutamate and GABA receptors at central synapses. *Curr Opin Neurobiol* **17**, 387–393.

Moss SJ & Smart TG (2001). Constructing inhibitory synapses. *Nat Rev Neurosci* **2**, 240–250.

Naldini L, Blomer U, Gage FH, Trono D & Verma IM (1996). Efficient transfer, integration, and sustained long-term expression of the transgene in adult rat brains injected with a lentiviral vector. *Proc Natl Acad Sci U S A* **93**, 11382–11388.

Nusser Z, Naylor D & Mody I (2001). Synapse-specific contribution of the variation of transmitter concentration to the decay of inhibitory postsynaptic currents. *Biophys J* **80**, 1251–1261.

Ochman H, Gerber AS & Hartl DL (1988). Genetic applications of an inverse polymerase chain reaction. *Genetics* **120**, 621–623.

Previtali SC, Quattrini A, Fasolini M, Panzeri MC, Villa A, Filbin MT, Li W, Chiu SY, Messing A, Wrabetz L & Feltri ML (2000). Epitope-tagged P_0 glycoprotein causes Charcot-Marie-Tooth-like neuropathy in transgenic mice. *J Cell Biol* **151**, 1035–1046.

Shevtsova Z, Malik JM, Michel U, Scholl U, Bahr M & Kugler S (2006). Evaluation of epitope tags for protein detection after *in vivo* CNS gene transfer. *Eur J Neurosci* **23**, 1961–1969.

Slimko EM, McKinney S, Anderson DJ, Davidson N & Lester HA (2002). Selective electrical silencing of mammalian neurons *in vitro* by the use of invertebrate ligand-gated chloride channels. *J Neurosci* **22**, 7373–7379.

Szybalski W, Kim SC, Hasan N & Podhajska AJ (1991). Class-IIS restriction enzymes – a review. *Gene* **100**, 13–26.

Tan EM, Yamaguchi Y, Horwitz GD, Gosgnach S, Lein ES, Goulding M, Albright TD & Callaway EM (2006). Selective and quickly reversible inactivation of mammalian neurons in vivo using the *Drosophila* allatostatin receptor. *Neuron* **51**, 157–170.

Terpe K (2003). Overview of tag protein fusions: from molecular and biochemical fundamentals to commercial systems. *Appl Microbiol Biotechnol* **60**, 523–533.

Tomic M, Sunjevaric I, Savtchenko ES & Blumenberg M (1990). A rapid and simple method for introducing specific mutations into any position of DNA leaving all other positions unaltered. *Nucleic Acids Res* **18**, 1656.

Trimmer JS & Rhodes KJ (2004). Localization of voltage-gated ion channels in mammalian brain. *Annu Rev Physiol* **66**, 477–519.

Wulff P, Goetz T, Leppa E, Linden AM, Renzi M, Swinny JD, Vekovischeva OY, Sieghart W, Somogyi P, Korpi ER, Farrant M & Wisden W (2007). From synapse to behaviour: rapid modulation of defined neuronal types with engineered $GABA_A$ receptors. *Nat Neurosci* **10**, 923–929.

Author contributions

M.S. and Y.F. generated the lentiviruses, performed the transduction of cells and analysed the data in cultures in Japan. K.M. performed the whole-cell patch-clamp recordings on cultured cells and analysed the data in Japan. M.D.E. carried out patch-clamp recordings in acute slices and analysed his data in Hungary. A.L. performed the immunohistochemical experiments in cortical sections and carried out the SDS-FRL experiments in Hungary. Z.N. and R.S. designed the project and drafted the article. All authors approved the final version of the manuscript.

Acknowledgements

This work was supported by a Fellowship from the Japan Society for the Promotion of Science to M.S.; a grant from Solution Oriented Research for Science and Technology (SORST), Japan Science and Technology Agency to R.S.; grants from the Ministry of Education, Culture, Sports, Science and Technology of Japan, Grants-in-Aid for Scientific Research on Priority Areas – Molecular Brain Science (18022043) to Y.F.; and Grants-in-Aid for Young Scientists (18680903) to K.M.; a Project Grant (090197/Z/09/Z) and an Equipment Grant (083484/Z/07/Z) from the Wellcome Trust; Hungarian National Office for Research and Technology-French National Research Agency TéT Fund (NKTH-Neurogen) to Z.N. Support from these foundations is gratefully acknowledged. We would like to thank Drs Peer Wulff and William Wisden for providing the $GABA_A$ receptor γ2-L subunit cDNA and for the $GABA_AR\gamma2^{77I}$lox mice, Dr Bernhard Luscher for the $GABA_AR\gamma_2^{+/-}$ mice, Profs Werner Sieghart and Jean-Marc Fritschy for the anti-γ2 antibodies and Dr Pavel Osten for plasmids for lentivirus.